Theor Chem Acc (2017) 136:41
DOI 10.1007/s00214-017-2069-z

REGULAR ARTICLE

A theoretical study of the $H_nF_{4-n}Si$:N-base (n = 1–4) tetrel-bonded complexes

Marta Marín-Luna[1,2] · Ibon Alkorta[2] · José Elguero[2]

Received: 10 November 2016 / Accepted: 30 November 2016 / Published online: 6 March 2017

Abstract Tetrel-bonded complexes of $H_nF_{4-n}Si$ with a N-base for n = 0–4 were explored by MP2 calculations. Configurations with H–Si···N and F–Si···N linear or nearly linear alignment in complexes were considered. Nine sp^3 hybridized nitrogen bases NH_3, NH_2Cl, NH_2F, $NHCl_2$, NCl_3, $NFCl_2$, NHF_2, NF_2Cl, NF_3 and nine sp ones $NCNH_2$, $NCCH_3$, NCOH, NP, NCCl, NCH, NCF, NCCN, N_2 have been studied. It is shown that binding energies of the complexes depend strongly on the nature of the base involved in the complex. Complexes with NH_3 bases present the highest binding energies. In the stronger complexes, the silicon molecules suffer important geometrical distortions. NBO and AIM methodologies have been applied in order to describe properly the intermolecular Si···N contact. F atoms in equatorial position at silicon acid provoke a deviation from linearity of the Si···N electron density bond path trajectory.

Published as part of the special collection of articles derived from the 10th Congress on Electronic Structure: Principles and Applications (ESPA-2016).

Electronic supplementary material The online version of this article (doi:10.1007/s00214-017-2069-z) contains supplementary material, which is available to authorized users.

✉ Marta Marín-Luna
mmarin@uvigo.es

✉ Ibon Alkorta
ibon@iqm.csic.es

[1] Departamento de Química Orgánica, Universidad de Vigo, Vigo, Spain

[2] Instituto de Química Médica, CSIC, Juan de la Cierva, 3, 27006 Madrid, Spain

Keywords Tetrel bond · σ-Hole · Nitrogen bases · Fluorosilanes · MP2 calculations

1 Introduction

Non-covalent interactions play important roles in supramolecular assemblies [1, 2] and in biological chemistry [3, 4]. Although most related published works focus on hydrogen bonds [5–8], there are other weak interactions that have attracted the attention of chemists [9, 10]. These interactions have been denoted as σ-hole bonds based on the positive character of the electrostatic potential surrounding an atom of groups 14–17 of the periodic table [11–14]. σ-Hole bonds are commonly known by the name of the periodic table group of the atom acting as Lewis acid in the interaction: tetrel [15–17] (group 14), pnicogen [18, 19] (group 15), chalcogen [15, 20–22] (group 16) and halogen [14, 23, 24] (group 17) bonds.

In this work we focus on tetrel bonds, particularly in those cases where the silicon atom acts as electron acceptor. The Si atom has been shown to establish stable weak interactions with N atoms [25–29]. For instance, an intramolecular Si···N interaction is responsible for the coloration in the solid-state of disylazobenzenes [30] and it is crucial to the structural conformation stability of *N*,*N*-dimethylaminopropyl silane [31], trifluorosilylhydrazines [32] and silatranes [33, 34]. Recently, the existence of cooperativity between linear chains of $(H_3TCN)_n$ and $(H_3TNC)_n$ complexes, with T=C and Si, connected by tetrel bonds has been described [35, 36].

In 2015, we reported a theoretical study of P···N pnicogen bonds in $F_{4-n}H_nP^+$:N-base with F-P···N linear or nearly linear [37, 38]. In this study, an exponential correlation between binding energies and P···N distances was

found for the complexes formed by different Lewis bases. The binding energies of these complexes increase in absolute value with the number of fluorine atoms in the molecule: $FH_3P^+ < F_2H_2P^+ < F_3HP^+ < F_4P^+$. A similar study on chalcogen bonded $F_{3-n}H_nS^+$:N-base has been reported [22].

Following a similar idea, here we explored 144 $F_{4-n}H_nSi$:N-base (n = 0–4) neutral complexes being the N-base monomers either sp^3-hybridized bases NH_3, NH_2Cl, NH_2F, $NHCl_2$, NCl_3, $NFCl_2$, NHF_2, NF_2Cl, NF_3 or sp bases $NCNH_2$, $NCCH_3$, NCOH, NP, NCCl, NCH, NCF, NCCN, N_2. Both possible X-Si···N linear disposition configurations with X = F or H have been considered (see Fig. 1 for the schematic representation of the complexes of H_2F_2Si). In order to describe the Si···N interaction, binding energies, geometrical parameters, electron densities, bond critical points and charge-transfer energies of the minima were computed in those systems with $F(H)_{ax}$-Si···N linear disposition.

2 Computational methods

The geometries of monomers and complexes have been fully optimized with the Gaussian 09 package [39] using the second order Møller–Plesset perturbation theory (MP2) [40] and the aug′-cc-pVTZ basis set [41]. This basis set is composed by the Dunning aug-cc-pVTZ [42] bases for the heavy atoms while removing the diffuse function from the H atoms. Harmonic frequency analyses have been performed to confirm that the geometry of the systems correspond to energetic minima.

Binding energies have been obtained as the difference between the energy of the complex and the sum of the energies of each monomer in its minimum geometry.

The electrostatic potentials of the isolated monomers have been calculated with the Gaussian-09 and analyzed with the Multiwfn 3.3.5 program [43] on the 0.001 au electron density isosurface to locate the position and value of the maxima critical points on the isosurface. The Molecular Electrostatic Potential Maps on the 0.001 au electron density isosurface have been plotted by using the Jmol program [44]. The electron density properties have been studied with the Atoms in Molecules (AIM) methodology [45–47] using the AIMAll program [48]. Bond critical points (BCPs) have been analyzed in terms of the electron density (ρ_{BCP}), its Laplacian ($\nabla^2\rho_{BCP}$) and the total electron energy density (H_{BCP}). The Natural Bond Orbital (NBO) method has been applied to analyze the charge transfer between occupied and empty orbitals. The NBO stabilization energies due to the orbital charge transfer were calculated at B3LYP/aug′-cc-pVTZ level on the previously optimized geometries (MP2/aug′-cc-pVTZ level), employing the NBO-6 program [49].

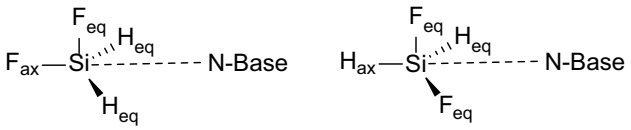

Fig. 1 Schematic representation of the F_2H_2Si:N-base complexes with F_{ax}–Si···N (*left*) and H_{ax}–Si···N (*right*) linear dispositions

3 Results and discussion

3.1 Monomers

Molecular electrostatic potential (MESP) of $H_nF_{4-n}Si$ (n = 0–4) acids have been analyzed and represented in Fig. 2 on the 0.001 au electron density isosurface. Four MESP maximum are found in each molecule associated with the σ-hole along the extension either of the Si–F or Si–H axis. In all cases, the MESP value of the σ-hole along the Si–F bond is larger than that involving H atom. A global analysis of the MESP representation shows that the values of both types of σ-holes, along Si–F or Si–H axes, increase as the number of F atoms does (Fig. 1). Linear correlations between the MESP value on the σ-hole and the number of F atoms are obtained with good to moderate statistical values (R^2 = 0.98 and 0.87 for the σ-holes of the Si–H and Si–F bonds, respectively). Based on these results, it is expected that the strongest interactions with N-bases occur with SiF_4 and, in a given molecule, the complexes associated to Si–F σ-holes should be stronger than those corresponding to the Si–H ones.

The MESP of the nitrogen bases shows a minimum on the 0.001 au electron density isosurface in the proximity of the nitrogen atom (Table 1). The values range between −0.063 for N≡C–NH_2 to −0.005 for NF_3. Thus, the complexes involving N≡C–NH_2 are expected to provide the strongest interactions with the silicon acids.

3.2 Complexes

Cartesian coordinates and molecular graphs of all dimers here studied are gathered in Table S1 of the ESM. A representation of the complexes $H_nF_{4-n}Si{:}NH_3$ is shown in Fig. 3. Complexes with SiF_4, $SiHF_3$, SiH_3F and SiH_4 present either C_{3v} or C_s symmetry, and those with SiH_2F_2 have always C_s symmetry. Note that the results obtained for the complexes of SiF_4, SiH_4 and SiH_3F (with F in axial position) with NCH are similar to those previously described by Grabowski [17].

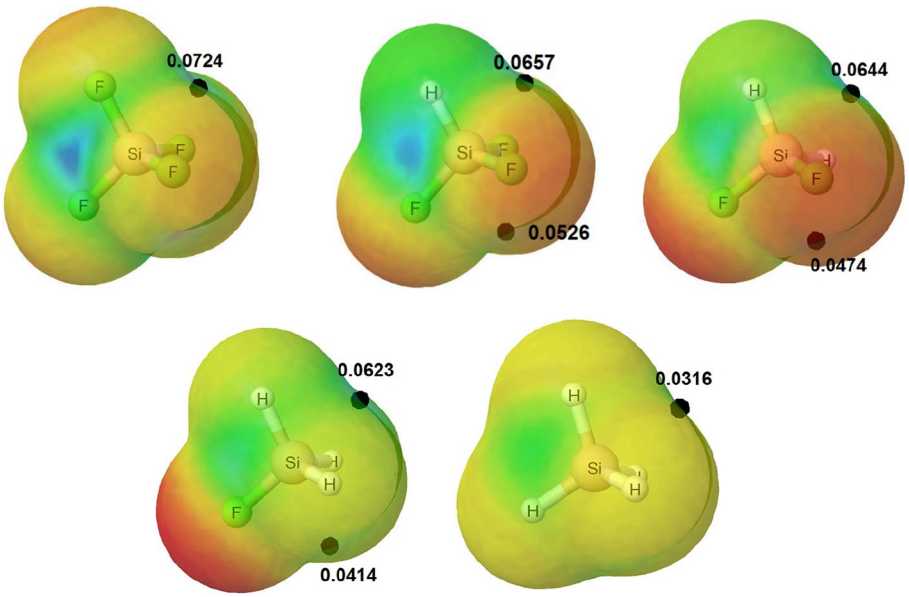

Fig. 2 Representation of MESP on the 0.001 au electron density isosurface of SiF_4 (*left top*), SiF_3H (*middle top*), SiF_2H_2 (*right top*), SiH_3F (*left bottom*) and SiH_4 (*right bottom*). *Color scale* is defined from −0.03 au (*red*) to 0.08 au (*blue*). *Black dots* indicate the location of the σ-hole and its value is given in au

Table 1 Minima of the nitrogen bases (au)

sp^3 bases		*sp* bases	
NH_3	−0.0595	N≡C–NH_2	−0.0632
$NClH_2$	−0.0439	N≡C–CH_3	−0.0607
NFH_2	−0.0455	N≡C–OH	−0.0572
NCl_2H	−0.0301	N≡P	−0.0500
NCl_3	−0.0189	N≡C–Cl	−0.0486
NF_2Cl	−0.0113	N≡C–H	−0.0509
NF_2H	−0.0268	N≡C–F	−0.0454
$NFCl_2$	−0.0160	N≡C–C≡N	−0.0319
NF_3	−0.0049	N≡N	−0.0136

Table 2 lists the binding energies (BEs) of all complexes and their Si···N distances. In a few dimers involving a *sp*-base, the minima found corresponds to the interaction of the CN triple bond with the σ-hole of the silicon derivatives and not are considered in the discussion (see Table S1 of the ESM).

The complexes have been divided in two subgroups depending on the hybridization of nitrogen of the base, sp^3 or *sp*, and are listed according to the decreasing order of the binding energies with SiF_4. In these complexes, the binding energies of sp^3 bases range between −9.1 and −45.0 kJ·mol^{-1}, being those with NH_3 and NF_3 the

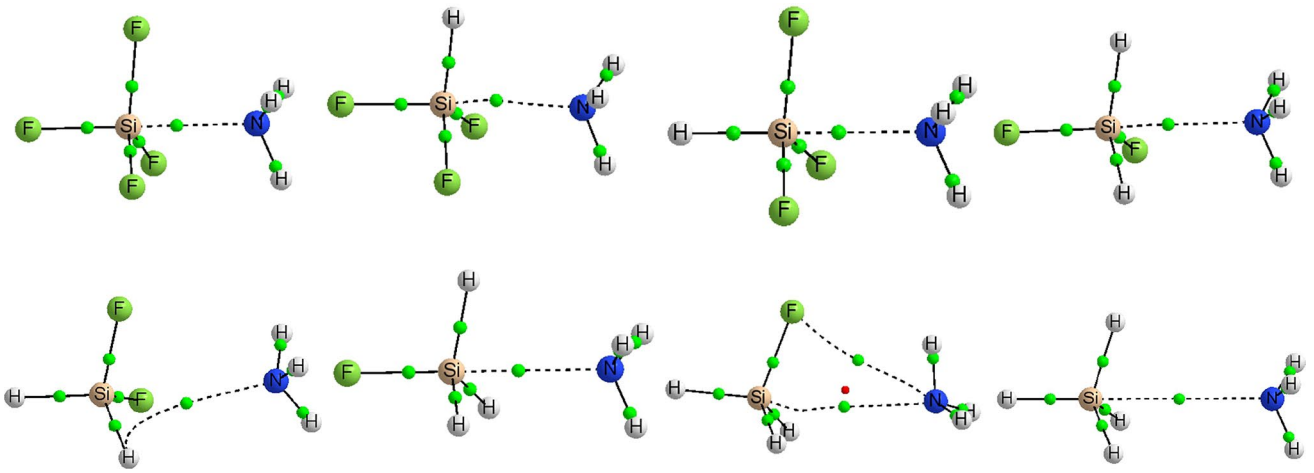

Fig. 3 Molecular graphs of $F_{4-n}H_nSi{:}NH_3$ complexes. *First row*, from left to right: $F_4Si{:}NH_3$, $F_3HSi{:}NH_3$ (F_{ax}), $F_3HSi{:}NH_3$ (H_{ax}), $F_2H_2Si{:}NH_3$ (F_{ax}). *Second row*, from left to right: $F_2H_2Si{:}NH_3$ (H_{ax}), $FH_3Si{:}NH_3$ (F_{ax}), $FH_3Si{:}NH_3$ (H_{ax}), $H_4Si{:}NH_3$

Table 2 Binding energies (kJ mol^{-1}) and Si···N intermolecular distances (Å) of complexes of $F_{4-n}H_nSi$ with nitrogen bases

Base	SiF_4		SiF_3H (F_{ax})		SiF_3H (H_{ax})		SiH_2F_2 (F_{ax})		SiH_2F_2 (H_{ax})		SiH_3F (F_{ax})		SiH_3F (H_{ax})		SiH_4	
NH_3	−45.0	2.074	−29.8	2.208	−25.0	2.104	−28.0	2.392	−16.2	2.996	−28.2	2.498	−14.6	3.084	−9.3	3.196
NH_2Cl	−26.0	2.217	−18.9	2.789	−15.0	2.958	−26.3	2.531	−17.5	2.932	−25.6	2.551	−16.2	3.020	−10.8	3.1432
NH_2F	−23.8	2.196	−15.8	2.881	−12.7	2.983	−22.6	2.632	−15.5	3.051	−21.9	2.567	−16.0	3.093	−8.1	3.218
$NHCl_2$	−20.2	2.874	−21.6	2.793	−15.2	3.040	−19.6	2.796	−17.1	2.942	−23.7	2.626	−13.6	3.049	−12.3	3.086
NCl_3	−20.1	2.947	−20.1	2.879	−16.3	3.062	−21.7	2.762	−16.9	2.982	−23.5	2.685	−16.5	2.949	−14.2	3.006
$NFCl_2$	−16.5	2.987	−15.2	2.958	−13.5	3.105	−17.3	2.859	−12.9	3.050	−18.4	2.746	−13.6	3.064	−10.8	3.101
NHF_2	−13.6	2.990	−14.5	3.011	−9.9	3.143	−11.1	3.000	−13.0	3.264	−14.4	2.794	−14.4	3.443	−6.5	3.282
NF_2Cl	−12.8	3.076	−12.5	3.088	−10.6	3.185	−11.4	2.983	−11.0	3.165	−13.2	2.862	−8.8	3.147	−7.9	3.245
NF_3	−9.1	3.187	−8.2	3.222	−7.9	3.273	−8.0	3.168	−7.6	3.280	−8.5	3.025	−7.0	3.319	−5.0	3.387
$NCNH_2$	−20.1	2.853	−20.7	2.907	−11.8	3.088	−22.1	2.834	–[a]		−22.8	2.743	–[a]		−9.5	3.219
$NCCH_3$	−19.4	2.881	−19.2	2.934	−11.4	3.100	−20.7	2.855	–[a]		−21.9	2.761	–[a]		−9.1	3.227
NCOH	−18.2	2.935	−18.8	2.970	−10.9	3.132	–[a]		–[a]		−20.4	2.798	–[a]		−8.8	3.238
NP	−17.9	2.924	−18.0	2.959	−11.2	3.132	−19.6	2.858	−12.6	3.139	−21.3	2.739	–[a]		−9.3	3.212
NCCl	−16.4	3.005	−16.3	3.027	−10.3	3.175	−17.4	2.945	–[a]		−18.3	2.840	–[a]		−8.4	3.264
NCH	−15.9	3.007	−15.7	3.038	−9.7	3.181	−16.7	2.956	−10.5	3.182	−17.8	2.847	–[a]		−7.7	3.285
NCF	−15.0	3.048	−15.0	3.067	−9.6	3.203	−15.8	2.987	–[a]		−16.5	2.890	–[a]		−7.6	3.293
NCCN	−13.1	3.115	−12.7	3.132	−9.3	3.247	−13.1	3.056	–[a]		−13.8	2.936	–[a]		−7.0	3.325
N_2	−7.6	3.300	−7.0	3.327	−5.9	3.399	−6.9	3.279	−5.8	3.387	−7.3	3.175	−5.3	3.405	−4.1	3.481

[a] These complexes present no Si–N_{LP} interaction

strongest and the weakest one, respectively. In the case of *sp* bases the strongest interaction is found with $NCNH_2$, with a BE of amount half of that with NH_3, −20.1 kJ·mol^{-1}. The weakest Si···N interaction is found with the N_2 base (−7.6 kJ·mol^{-1}). The extreme binding energy in each of the two N-bases series (sp^3 and *sp*) are in agreement with the values of the MESP of isolated bases but not when they are considered in a unique set since the MESP minima of $NCNH_2$ is more negative than that of NH_3 and the one of N_2 is larger than that of NF_3. These results points toward the possibility of secondary interactions especially in the complexes with sp^3 bases [50, 51].

An analysis of the data of Table 2 shows that for a given complex, the stabilization when the atom in axial position is a F atom is higher than when it is a H atom, except in the case of the SiH_2F_2:NHF_2 and SiH_3F:NHF_2 complexes. For the former case the conclusion is the opposite and in the last case both BEs are equal (−14.4 kJ·mol^{-1}). Concerning the Lewis acid, in general the rank of the BEs of each base is similar to that of the complexes with SiF_4. Thus, linear correlations are found between the MESP minima of the N-base and the binding energy for the complexes of the *sp* bases for each given Lewis acid ($R^2 > 0.9$). Attempts to find a similar correlation for the sp^3 bases provide poor correlation coefficients ($R^2 < 0.8$).

There is not a clear relation between the binding energies and the number of F atoms in the Lewis acid, as occurred in the previous work with phosphines [37]. Nevertheless, for a given base, the strongest interactions are with SiH_3F_{ax} with some exceptions: the complexes of NH_3, NH_2F, NF_3 and N_2 with SiF_4 present higher BE, while for NH_2Cl and NHF_2 are those with SiH_2F_2 (F_{ax}) and with SiF_3H (F_{ax}), respectively. In the case of the *sp* bases, good linear correlations ($R^2 > 0.96$) are found for the different complexes, except for those with N_2.

The Si···N intermolecular distances are also reported in Table 2. The calculated value for SiF_4:NH_3 is very close to the experimental microwave one (2.090 Å) [26]. The distances range from 2.074 in SiF_4:NH_3 to 3.481 Å in SiH_4:N_2, which correspond to the highest and lowest BE, respectively. Curiously, gaps in the Si···N distances are observed for the complexes of SiF_4, SiF_3H (F_{ax}) and SiF_3H_{ax} complexes between 2.217–2.853, 2.208–2.789 and 2.104–2.958 Å, respectively. The histogram of the Si···N distances for all the complexes (Fig. 4) shows that the most frequent distances are between 3.0 and 3.2 Å with 44 cases, being the average value 3.00 Å.

As expected, BE increases as the Si···N intermolecular distances decrease. Several correlations are found between BE and Si···N distances. Figure 5a shows these trendlines for complexes with sp^3 nitrogen bases whereas in Fig. 5b those with *sp* bases are illustrated. Note that only complexes in which a F atom is in axial positions of the Lewis acid monomer have been included in the regression analysis. Complexes with sp^3 bases cover a range of distances larger than those with *sp* bases. In the case of sp^3 bases, trendlines of SiH_3F complexes are exponential while they are linear in $SiHF_3$ and SiH_2F_2 systems, with correlation coefficients of

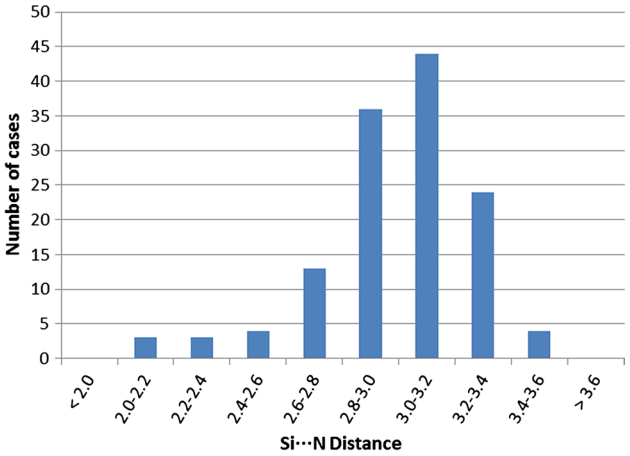

Fig. 4 Histogram of the Si···N distances (Å) in all the calculated complexes

0.935, 0.926 and 0.958 respectively. These three trendlines cross in a point around 2.6 Å. A R^2 lower than 0.8 is found in the case of SiF_4 containing systems and the associated trendline is omitted. In the case of *sp* nitrogen bases the exponential correlations show R^2 values of 0.963, 0.983, 0.987 and 0.987 for systems with SiF_4, $SiHF_3$, SiH_2F_2 and SiH_3F respectively. Note that for a particular BE the Si···N distances vary in order: $SiH_3F < SiH_2F_2 < SiF_4 < SiHF_3$. The fact that, for a given silicon derivative, the correlations involving sp^3-bases are worse than those with *sp*-bases may indicate that the former present secondary interactions in addition to tetrel bonds, influencing their properties.

Interactions with nitrogen bases provoke variations in internal geometries of silicon derivatives. Table 3 lists Si–F_{ax}, Si–H_{ax} bond distances and relevant angles F_{ax}–Si–H_{eq}, H_{ax}–Si–F_{eq} and F_{ax}–Si–F_{eq} or H_{ax}–Si–F_{eq} of the complexes and of the isolated monomers. Let us start with complexes with F in position axial of the silicon acid. As it can be seen in Table 3 a stretch of bonds respect to the ones in isolated monomers is observed. This Si–F_{ax} bond elongation is higher as BEs increase. For instance, in SiF_4:NH_3 (BE = –45 kJ·mol^{-1}) and SiF_4:N_2 (BE = –7.6) the Si–F_{ax} distance is 1.612 and 1.576 Å which is 0.038 and 0.002 Å longer than Si–F bond length in SiF_4. The Si–F_{ax} elongation correlates with the Si···N distances when the complexes are divided according to the bases (sp^3 and *sp*). The R^2 are between 0.94 and 0.96 for the *sp* and between 0.98 and 0.81 for the sp^3 (Fig. S1).

Modification of internal F–Si–F and F–Si–H bond angles is observed upon complexation; these angles are lower in complexes than in the isolated monomers being the variation more significant in complexes that present higher BE. For instance, the F_{ax}–Si–F_{eq} angle of SiF_4 complexes with NH_3 decrease around 13° respect to the isolated SiF_4. In contrast, the F–Si–F angle of complexes of SiF_3H (F_{ax}) with NCCl, NCF and NCCN and F–Si–H of SiH_2F_2:NCOH are slightly larger, around 1° and 0.2°, than in the isolated monomer.

Analogous geometrical changes are observed in complexes in which H atom is axial in the silicon derivatives. In these cases the elongation percentage of Si–H_{ax} is lower than that associated to Si–F_{ax}. In the former case, the percentage rises up until 1.15% while for the latter ones, it rises up to 2.41%. For instance, in SiF_3H:NH_3 the elongation of Si-F_{ax} is of 2.20% and of 1.15% of Si–H_{ax}. In relation to the angles studied, angles are lower in complexes than in the isolated monomers.

Natural bond orbital (NBO) methodology was applied to analyze the charge-transfer energy [E(2)] between monomers. Charge transfer from the N-base to Si–X_{ax} bond stabilized the tetrel bond. Relevant E(2) are shown in Tables S2 of ESM. In two cases, SiF_4:NH_3, SiF_3H_{ax}:NH_3, the NBO program considers these complexes as just one molecule and the calculations of the intermolecular E(2) were not possible. In the rest of complexes, as expected, there is a charge transfer from the lone pair of N atom (N_{LP})

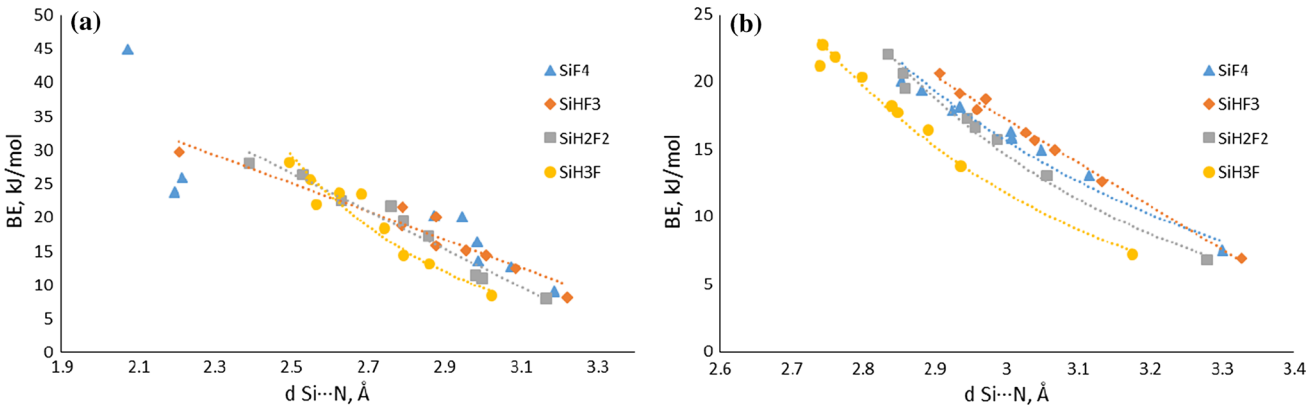

Fig. 5 Negative Binding energy versus Si···N distances of $F_{4-n}H_nSi$ with F in axial position and sp^3 bases (**a**) or *sp* bases (**b**)

Table 3 Relevant variation of bond distances (Å)

Base	SiF_4		SiF_3H (F_{ax})	SiH_2F_2 (F_{ax})	SiH_3F (F_{ax})		SiF_3H (H_{ax})		SiH_2F_2 (H_{ax})	SiH_3F (H_{ax})	SiH_4	
	Si–F_{ax}	Si–F_{eq}	Si–F_{ax}	Si–F_{ax}	Si–F_{ax}	Si–H_{eq}	Si–H_{ax}	Si–F_{eq}	Si–H_{ax}	Si–H_{ax}	Si–H_{ax}	Si–H_{eq}
NH_3	0.038	0.036	0.046	0.053	0.067	0.000	0.017	0.039	0.006	0.009	0.007	−0.001
NH_2Cl	0.028	0.021	0.023	0.042	0.058	0.003	0.004	0.005	0.005	0.007	0.006	0.001
NH_2F	0.027	0.020	0.021	0.039	0.057	0.004	0.004	0.005	0.003	0.006	0.005	0.001
$NHCl_2$	0.007	0.003	0.020	0.034	0.053	0.000	0.003	−0.001	0.004	0.007	0.005	0.000
NCl_3	0.005	0.001	0.017	0.032	0.049	0.001	0.002	0.001	0.003	0.006	0.004	0.001
$NFCl_2$	0.004	0.001	0.016	0.030	0.047	0.002	0.002	0.002	0.002	0.005	0.003	0.001
NHF_2	0.005	0.002	0.016	0.031	0.048	−0.002	0.002	−0.002	0.001	0.003	0.003	−0.001
NF_2Cl	0.002	0.001	0.014	0.028	0.045	0.000	0.002	0.000	0.002	0.005	0.002	0.000
NF_3	0.001	0.001	0.013	0.026	0.043	0.001	0.001	0.000	0.001	0.004	0.001	0.001
$NCNH_2$	0.012	0.001	0.023	0.039	0.057	−0.002	0.005	−0.001	–[a]	–[a]	0.007	−0.001
$NCCH_3$	0.011	0.001	0.023	0.038	0.056	−0.001	0.005	−0.001	–[a]	–[a]	0.006	−0.001
NCOH	0.010	0.000	0.021	–[a]	0.055	−0.002	0.004	−0.001	–[a]	–[a]	0.006	−0.001
NP	0.009	0.001	0.021	0.036	0.055	−0.001	0.004	0.000	0.004	–[a]	0.006	−0.001
NCCl	0.008	0.000	0.020	0.035	0.052	−0.001	0.004	0.000	–[a]	–[a]	0.005	−0.001
NCH	0.008	0.000	0.020	0.035	0.052	−0.001	0.004	−0.001	0.004	–[a]	0.005	−0.001
NCF	0.007	0.000	0.019	0.033	0.051	−0.001	0.003	−0.001	–[a]	–[a]	0.005	0.000
NCCN	0.004	0.000	0.016	0.031	0.048	0.000	0.003	0.000	–[a]	–[a]	0.003	0.000
N_2	0.002	0.000	0.013	0.027	0.043	0.000	0.001	0.000	0.002	0.004	0.002	0.000

[a] These complexes present no Si-N_{LP} interaction

of the base toward antibonding σ * SiX_{ax} orbital. In addition, charge transfer from N_{LP} to antibonding Si–F_{eq} and Si–H_{eq} orbitals is found. In all complexes $N_{LP} \rightarrow$ σ * SiF_{ax} charge-transfer energy is always dominant respect to $N_{LP} \rightarrow$ σ * SiF_{eq} or $N_{LP} \rightarrow$ σ * SiH_{eq}. In addition, the values of E(2) are affected by the number of fluorine atoms in the molecule. As can be seen in Fig. 6a, exponential relationships are found between E(2) $N_{LP} \rightarrow$ σ * SiF_{ax} and the N···Si distance for the complexes of each silicon derivative with the *sp*-bases. The smallest values correspond to those of the SiF_4 complexes, and they steadily increase as the number of F atoms in the molecule decreases.

A similar trend is observed for the $N_{LP} \rightarrow$ σ * SiF_{eq} charge-transfer energy Fig. 6b, but now the range of energies is about 5 times smaller than for the $N_{LP} \rightarrow$ σ * SiF_{ax} ones. In addition, it is observed that in those cases that show $N_{LP} \rightarrow$ σ * SiF_{eq} and $N_{LP} \rightarrow$ σ * SiH_{eq}, the former is always larger than the latter.

Electron density properties at the Si···N bond critical point (BCP) have been analyzed by means of atoms

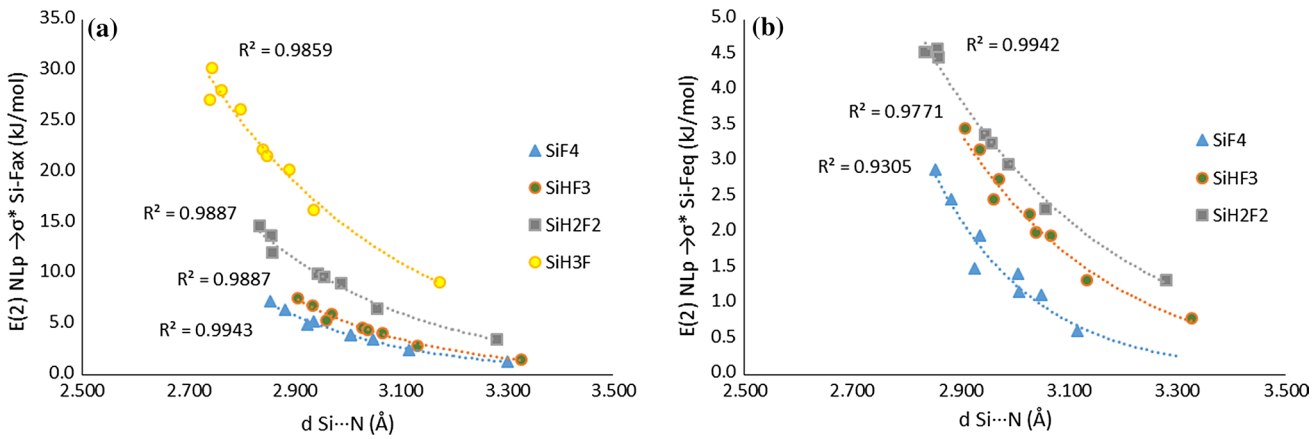

Fig. 6 **a** E(2) $N_{LP} \rightarrow$ σ * SiF_{ax} versus N···Si distance and **b** E(2) $N_{LP} \rightarrow$ σ * SiF_{ax} versus N···Si distance for *sp* complexes

in molecules (AIM) methodology. The electron density, ρ_{BCP}, its Laplacian, ($\nabla^2\rho_{BCP}$), and the total electron energy density, H_{BCP}, at the intermolecular Si···N BCPs are gathered in Table S3. A critical point at Si···N bond is found in most of the complexes. However, the influence of F atoms in equatorial position of the acid is significant on the trajectory of the intermolecular bond paths. In some systems with F atoms in equatorial position at silicon acid, an intermolecular bond path F_{eq}···N or H_{eq}···N appears while the direct Si···N bond path is absent (see Molecular Graphs in the ESM). Thus, complexes with SiF_4 acid and sp^3 bases: NH_3, NH_2Cl, NH_2F and NCl_3 show a BCP at Si···N but not in the rest of systems. For complexes with SiF_3H acid, only those with NH_3 base present a BCP at Si···N. While a similar BCP is found in almost all complexes with SiH_2F_2 when F is axial, no Si···N BCPs are found for complexes with H axial. In cases with SiH_3F, when F atom is axial, all complexes show a BCP at Si···N, but this is found only in three complexes when H atom is situated in axial position. All complexes with SiH_4 show a BCP at Si···N contact except with $NHCl_2$.

Ranges of values of electron density properties at Si···N contact of complexes are listed in Table 4. Complexes are divided taking into account the nature of the located atom in axial position in the silicon acid. The range of ρ_{BCP} is greater for complexes with H_{ax} than those with F_{ax}. Both complex types present positive Laplacian, while in the case of complexes with F axial some of them have H_{BCP} negative, and those with H_{ax}, H_{BCP} is always positive. Complexes with H_{BCP} negative are those formed with strong sp^3 bases and present short Si···N distances (see ESM). Remember that positive Laplacian is found in covalent Si–N bonds as for instance $H_3Si–NH_2$ ($\nabla^2\rho_{BCP} = +0.615$ au).

We have found an exponential correlation between ρ_{BCP} and Si···N distance. This relationship is shown in Fig. 7a and presents a R^2 of 0.984. This type of correlation has been reported for other types of weak interactions [52–58]. In addition, Fig. 7b displays the variation of H_{BCP} as function of the Si···N distance. It is important to note that for complexes with Si···N distances lower than 2.8 Å, the H_{BCP} turns negative, indicating a partial covalent character of that bond in those complexes [59].

4 Conclusions

In summary, we have studied a total of 144 tetrel-bonded complexes of the type $F_{4-n}H_nSi$···N-bases (n = 0–4) with a X–Si···N linear or nearly linear alignment. Some of the complexes with *sp* hybridized N-bases evolve toward the CN π systems acting as electron donor instead of the nitrogen lone pair. The computed binding energies of complexes range between −45.0 and −7.6 kJ mol^{-1}, being the SiF_4:NH_3 complex the most stable. The Si-N distances in the complexes range between 2.07 and 3.48 Å. Exponential correlations are found between the binding energy and the intermolecular distances.

The complex formation provokes modifications in internal geometries of the silicon acid such as elongation of

Table 4 Range of electron density properties at Si···N BCP

	F axial			H axial		
	ρ_{BCP}	$\nabla^2\rho_{BCP}$	H_{BCP}	ρ_{BCP}	$\nabla^2\rho_{BCP}$	H_{BCP}
Min	0.0054	0.0212	−0.0241	0.0041	0.0158	0.0005
Max	0.0617	0.1971	0.0011	0.0860	0.1769	0.0010

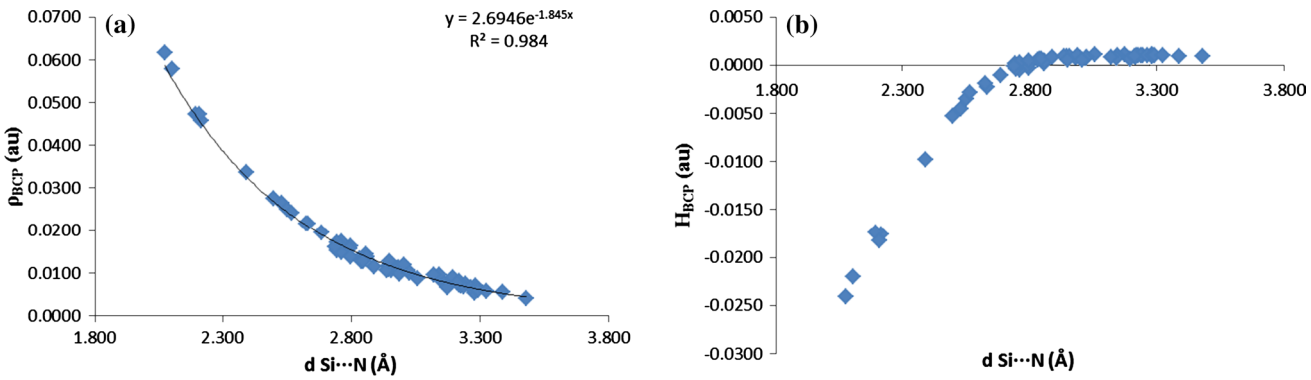

Fig. 7 **a** Electron density (ρ_{BCP}) versus Si···N distance and **b** total electron energy density (H_{BCP}) versus Si···N distance

Si–X_{ax} bond and a decrease in the X_{ax}–Si–F_{eq} and X_{ax}–Si–H_{eq} bond angles (X = F or H). The elongation of the Si–F_{ax} bonds correlates with the intermolecular distances found in the complexes.

Based on the NBO method, the complexes are stabilized by a $N_{LP} \rightarrow \sigma^* SiX_{ax}$ charge transfer and by a secondary $N_{LP} \rightarrow \sigma^* SiX_{eq}$ one. The values of such stabilizations correlate exponentially with the intermolecular distance.

Atom in molecules analysis shows the presence of Si···N bond paths in most of the complexes. In some cases, the presence of F atoms in equatorial position produces a deviation of the bond path ending it in one of the atoms bonded to the silicon (F_{eq} or H_{eq}). An exponential correlation between the electron density at the Si···N bond critical point and the intermolecular Si···N distance has been found. The values of the Laplacian and total electron density at the BCP with strong sp^3 bases indicate that they have partial covalent character.

Acknowledgements This work was carried out with financial support from the Ministerio de Economía y Competitividad (Project No. CTQ2015-63997-C2-2-P) and Comunidad Autónoma de Madrid (Project FOTOCARBON, ref S2013/MIT-2841). Computer, storage and other resources from the CTI (CSIC) are gratefully acknowledged.

References

1. Lehn J-M (2002) Science (Washington, DC, USA) 295(5564):2400
2. Badjic JD, Nelson A, Cantrill SJ, Turnbull WB, Stoddart JF (2005) Acc Chem Res 38(9):723
3. Yeagle PL (2014) Biochim Biophys Acta Biomembr 1838(6):1548
4. Cerny J, Hobza P (2007) Phys Chem Chem Phys 9(39):5291
5. Bernstein J, Davis RE, Shimoni L, Chang N-L (1995) Angew Chem Int Ed Engl 34(15):1555
6. Prins LJ, Reinhoudt DN, Timmerman P (2001) Angew Chem Int Ed 40(13):2382
7. Steiner T (2002) Angew Chem Int Ed 41(1):48
8. Grabowski SE (2006) Hydrogen bonding—new insights. Challenges and advances in computational chemistry and physics, vol 3. Springer Netherlands, Amsterdam
9. Singh SK, Das A (2015) Phys Chem Chem Phys 17(15):9596
10. Schreiner PR, Chernish LV, Gunchenko PA, Tikhonchuk EY, Hausmann H, Serafin M, Schlecht S, Dahl JEP, Carlson RMK, Fokin AA (2011) Nature (London, UK) 477(7364):308
11. Murray JS, Lane P, Politzer P (2009) J Mol Model 15(6):723
12. Murray JS, Riley KE, Politzer P, Clark T (2010) Aust J Chem 63(12):1598
13. Politzer P, Murray JS, Concha MC (2008) J Mol Model 14(8):659
14. Politzer P, Murray JS, Clark T (2013) PCCP 15(27):11178
15. Azofra LM, Scheiner S (2015) J Chem Phys 142(3):034307
16. Bauzá A, Mooibroek TJ, Frontera A (2013) Angew Chem Int Ed 52(47):12317
17. Grabowski SJ (2014) PCCP 16(5):1824
18. Del Bene JE, Alkorta I, Elguero J (2015) The pnicogen bond in review: structures, binding energies, bonding properties, and spin–spin coupling constants of complexes stabilized by pnicogen bonds. In: Scheiner S (ed) Noncovalent forces. Challenges and advances in computational chemistry and physics, vol 19. Springer, Berlin. doi:10.1007/978-3-319-14163-3_8
19. Scheiner S (2013) Acc Chem Res 46(2):280
20. Esrafili MD, Mohammadian-Sabet F (2015) Chem Phys Lett 628:71
21. Esrafili MD, Mohammadian-Sabet F (2015) J Mol Model 21(3):1
22. Esrafili MD, Mohammadian-Sabet F (2016) Chem Phys Lett 645:32
23. Metrangolo P, Resnati G (2015) Halogen bonding I. Impact on materials chemistry and life sciences. Topics in current chemistry, vol 358. Springer, Berlin
24. Politzer P, Lane P, Concha MC, Ma Y, Murray JS (2007) J Mol Model 13(2):305
25. Alkorta I, Rozas I, Elguero J (2001) J Phys Chem A 105(4):743
26. Ruoff RS, Emilsson T, Jaman AI, Germann TC, Gutowsky HS (1992) J Chem Phys 96(5):3441
27. Urban RD, Rouillé G, Takami M (1997) J Mol Struct 413:511
28. Alkorta I, Elguero J, Fruchier A, Macquarrie DJ, Virgili A (2001) J Organomet Chem 625(2):148
29. Rossi AR, Jasinski JM (1990) Chem Phys Lett 169(5):399
30. Yamamura M, Kano N, Kawashima T, Matsumoto T, Harada J, Ogawa K (2008) J Org Chem 73(21):8244
31. Hagemann M, Berger RJF, Hayes SA, Stammler H-G, Mitzel NW (2008) Chem A Eur J 14(35):11027
32. Vojinović K, McLachlan LJ, Hinchley SL, Rankin DWH, Mitzel NW (2004) Chem A Eur J 10(12):3033
33. Marín-Luna M, Alkorta I, Elguero J (2015) J Organomet Chem 794:206
34. Korlyukov AA, Lyssenko KA, Antipin MY, Kirin VN, Chernyshev EA, Knyazev SP (2002) Inorg Chem 41(20):5043
35. Marin-Luna M, Alkorta I, Elguero J (2016) J Phys Chem A 120(4):648
36. Esrafili MD, Mohammadirad N, Solimannejad M (2015) Chem Phys Lett 628:16
37. Del Bene JE, Alkorta I, Elguero J (2015) J Phys Chem A 119(22):5853
38. Bene JED, Alkorta I, Elguero J (2015) J Phys Chem A 119(12):3125
39. Frisch MJ, Trucks GW, Schlegel HB, Scuseria GE, Robb MA, Cheeseman JR, Scalmani G, Barone V, Mennucci B, Petersson GA et al (2009) Gaussian IWC. Gaussian-09, Revision A.01
40. Møller C, Plesset MS (1934) Phys Rev 46(7):618
41. Papajak E, Zheng J, Xu X, Leverentz HR, Truhlar DG (2011) J Chem Theory Comput 7(10):3027
42. Kendall RA, Dunning TH, Harrison RJ (1992) J Chem Phys 96(9):6796
43. Lu T, Chen F (2012) J Comput Chem 33(5):580
44. Jmol (2013) An open-source java viewer for chemical structures in 3D vhwjoaS
45. Bader RFW (1990) Atoms in molecules: a quantum theory. Oxford University Press, Oxford
46. Popelier PL (2000) Atoms in molecules: an introduction. Prentice Hall, London
47. Matta CF, Boyd RJ (2007) The quantum theory of atoms in molecules: from solid state to DNA and drug design. WILEY-VCH, Weinham
48. AIMAll (Version 14.11.23) TAK, TK Gristmill Software, Overland Park KS, USA, 2014 (aim.tkgristmill.com)
49. Glendening ED, Landis CR, Weinhold F (2013) NBO 6.0: natural bond orbital analysis program. J Comput Chem 34(16):1429–1437
50. Murray JS, Concha MC, Politzer P (2011) J Mol Model 17(9):2151
51. Politzer P, Murray JS, Clark T (2015) J Mol Model 21(3):52

52. Knop O, Boyd RJ, Choi SC (1988) J Am Chem Soc 110(22):7299
53. Gibbs GV, Hill FC, Boisen MB, Downs RT (1998) Phys Chem Miner 25(8):585
54. Espinosa E, Alkorta I, Elguero J, Molins E (2002) J Chem Phys 117(12):5529
55. Alkorta I, Barrios L, Rozas I, Elguero J (2000) THEOCHEM 496(1–3):131
56. Knop O, Rankin KN, Boyd RJ (2001) J Phys Chem A 105(26):6552
57. Mata I, Molins E, Alkorta I, Espinosa E (2007) J Phys Chem A 111(28):6425
58. Mata I, Alkorta I, Molins E, Espinosa E (2010) Chem A Eur J 16(8):2442
59. Rozas I, Alkorta I, Elguero J (2000) J Am Chem Soc 122(45):11154